Electronic Supplementary Material (ESI) for Physical Chemistry Chemical Physics.
This journal is © the Owner Societies 2016

Supplementary Material for:-

A theoretical study of the atmospherically important radical-radical reaction BrO + HO_2; the product channel $O_2(a^1\Delta_g)$ + HOBr is formed with the highest rate.

Ronald Chow [a], Daniel K.W. Mok [a], Edmond P. F. Lee *[a],[b], and John M. Dyke *[b]

[a] Department of Applied Biology and Chemical Technology, Hong Kong Polytechnic University, Hung Hom, Hong Kong

[b] School of Chemistry, University of Southampton, Highfield, Southampton SO17 1BJ, United Kingdom e-mail epl@soton.ac.uk; jmdyke@soton.ac.uk

Table S1.

Heats of formation ($\Delta H_{f,298K;}$ 0 K values in square brackets; best computed values in *italics*) used for calculating the reaction enthalpy (ΔH_{298K}^{RX}) of the BrO + HO_2 reaction channels (1a,1b, 2,3 and 4)

kcal.mol^{-1}	$\Delta H_{f,298K}$	Reference	Remarks
BrO	30.8	Grant2010	from atomization energies at R/UCCSD(T)/CBS+CV+SR+SO)
	[32.6]	As above	
	[31.4]	Orn2007	UCCSD(T)/CBS+CV+SO+rel+T+TQ from Peterson2006
	29.6± 0.4	Peterson2006	from computed D_0 at UCCSD(T)/CBS+CV+SO+rel+T+TQ
	29.5±0.1	Kim2006	ion imaging D_0; quoted in Sander2011
	[31.3±0.1]	As above	
	30.4±1.0	Den2004	CCSD(T)+CV+T+SO+rel
	30.2±0.4	Wil1999	FT-UV D_0; quoted in Canneaux2012 suppl.material
	30.1±0.4	JANAF1998	
	28.6±1.4	Bed1997	Quoted in Aran1997
	30.4±2	Orl1996	average from most direct measurements
	30.1±0.6	JANAF1996	Quoted in Burcat2010
	30.1±0.7		(average of all 298 K values, except Orl1996)
HO_2	2.85±0.05	Ganyecz2015	a thermo-chemical network, 14 experimental and 7 theoretical reaction enthalpies
	[3.55±0.05]	Ganyecz2015	(as above)
	2.84±0.05	*Ganyecz2015*	*CCSDTQP/CBS+SR+DBOA*
	2.93±0.04	ATcT2014	ATcT; quoted in Ganyecz2015
	2.7±0.9	Gold2012	RQCISD(T)/cc-PV∞QZ//B3LYP/6-311++G(d,p) + bond additivity correction; previous values: 0.5 to 3.0 kcal/mol
	2.9	Ruscic2011	Quoted in Gold2012
	3.3	Silva2011	No reference given
	3.17	Karton2011	using W4.2 TAE_{0K}=165.98kcal/mol and CODATA $\Delta H_{f,298K}$'s
	2.94±0.06	Burcat2010	ATcT
	[3.61±0.55]	Csaszar2010	NEAT
	2.91±0.05	Grant2009	ATcT; quoted in Ganyecz2015
	2.96±0.14	Karton2009	W4.2; quoted in Burcat2010, Ganyecz2015
	2.91±0.05	Harding2008	ATcT; quoted in Grant2009
	3.0±0.2	Feller2008	UCCSD(T)/CBS(Q;5)+CV+SR+SO; quoted in Grant2009, Ganyecz2015
	2.94±0.06	Ruscic2006	ATcT; quoted in Karton2009, Sander2011, Ganyecz2015
	[3.58±1.5]	Tajti2004	ATcT; quoted in Csaszar2010
	2.96±0.10	Flowers2004	CCSD(T)/aug-cc-pCV5Z; quoted in Ganyecz2015

	[3.97]	Henry2002	G3X-RAD
	3.2±0.5	Ramond2002	Photoelectron detachment; quoted in Ganyecz2015
	3.3±0.8	Litorja1998	photoionization mass spectrom.; quoted in Ganyecz2015
	2.32±0.72	JANAF1998	
	4.0±0.6	Esp1993	MP4/TZ(2df,p)+post-MP4 correction
	3.0	Hill1984	From T dependent rate coefficients; quoted in Burcat2010
	3.5±1.0	Shum1983	Review; quoted in Ganyecz2015
	3.0±0.5		(averaged of all 298 K values, except the smallest JANAF1998, the largest MP4 Esp1993 values and earlier values quoted in Ganyecz2015 with large uncertainties)
HOBr	*-15.3±0.60*	*Den2006*	*CCSD(T)+CV+T+SO+rel; quoted by Sandar2011JPL*
	[-11.4±0.4]	Joe2001	Thermochemical cycle
	-15.2±1.1	Esp1999	Best average theoretical value
	-14.5	Esp1999	CCSD(T)/CBS
	-19.4	Jur1999	MP4/CBS//MP2/6-31G(d')
	[-14.8]	Jur1999	B3LYP/6-311G(3df,3pd); recommended
	-18.2	Jur1999	B3LYP/6-311G(3df,3pd)
	-17.5	Mes1999	G2
	-14.5±0.3	Has1997	Recommended value; quoted in Canneaux2012 suppl. Material and Sander2011 JPL-NASA
	-14.3±1	Loc1996	Quoted and favoured by Orn2007 & San2001; quoted by Den2006
	[-11.8±1]	As above	
	-14.1±2	Orl1996	Average from most direct measurements
	-15.8	Gre1996	Bond additivity; quoted in Mes1999
	[-10.9±1]	JANAF1994	Quoted in Jur1999, Fran1994, Guha1999
	-14±2	DeM1994	Quoted in Esp1999
	-13.59±0.42	Rus1994	Corrected for ΔH_f(OH) given in San2001; quoted in Has1997
	-13.9±0.5	Rus1994	Quoted by Den2006 as the accepted value
	-14.2	McG1994	G2; quoted in San2001
	-14.4±0.9		(average of 298 K values >-13.5 and <-15.5 kcal/mol)
O_2 ($\tilde{X}^3\Sigma_g^-$)	0		By definition for the ground $\tilde{X}^3\Sigma_g^-$ electronic state.
O_2 ($\tilde{a}^1\Delta_g$)	22.54±0.01	Huber1998	Infrared solar spectrum; quoted in Sandar2011 JPL
	22.54		
HBr	-8.64±0.04	Burcat2010	ATcT
	-8.6	*Feller2003*	*CCSD(T)/CBS with aug-cc-pVnZ where n = T,Q, and 5*
	-8.71	JANAF1998	Absorption spectrum

	-8.67±0.04	Cox1989	CODATA
	-8.67±0.04	Gurvich1989	Quoted in Burcat2010
	-8.66±0.06		(average of all 298 K values)
O_3	38.1	Mor2012	ccCA
	34.9	Mor2012	G3
	33.88±0.04	Burcat2010	ATcT
	35.4	Burcat2010	G3MP2B3
	36.8	*Fab2005*	*W1U; quoted in Mor2012 and Burcat2010*
	33.87±0.01	Ruscic2004	ATcT; quoted in Sandar2011JPL
	36.8	*Haw2002*	*CCSD(T)/CBS+SR//B3LYP/6-31G(2df,p); quoted in Mor2012*
	33.89	Tan1999	VUV laser-induced fluorescence spectroscopy
	34.1	JANAF1998	calorimetric measurements
	33.9±0.5	Gurvich1991	Calorimetric measurement of the enthalpy of dissociation (O_3)
	33.9	Gurvich1989	Quoted in Burcat2010
	34.7±2.0		(average of all 298 K values; except the ccCA value)
OH	8.96±0.01	Ruscic2015; Ruscic2014	ATcT (agree with earlier values in Ref. 30 and 31)
	8.9±0.9	Gold2012	RQCISD(T)/cc-PV∞QZ//B3LYP/6-311++G(d,p) + bond additivity correction; previous values: 8.9 to 9.4 kcal/mol
	9.0	Ruscic2011	ATcT; quoted in Gold2012
	8.89±0.09	Ruscic2012	Position ion cycle (photoionization and photoelectron measurements) for Ruscic2001
	8.93±0.01	Burcat2010	ATcT
	8.91± 0.07	Ruscic2002	Recommended value at 298 K; quoted in Burcat2010
	[8.85±0.07]	Ruscic2002	Recommended value at 0 K
	[8.85±0.18]	Ruscic2002	CCSD(T)(FC)/CBS with unc-cc-pVnZ basis set; FCI for further corrections in the atomization energy.
	[8.85±0.18]	Ruscic2002	PIMS experiment
	[8.86±0.18]	Ruscic2002	PFI-PE30 experiment
	[8.83±0.12]	Ruscic2002	PFI-PEPICO experiment
	[8.92±0.03]	Ruscic2002	photodissociation of water
	8.92±0.16	Herbon2002	Shock tube measurement
	[8.68]	Henry2002	W2
	9.319	JANAF1998	
	[9.18±0.29]	JANAF1998	Spectroscopic determination
	[8.83±0.18]	Wie1992	Positive ion cycle
	8.89±0.09	Gurvich1991	D_0(H-OH)

	[9.35±0.05]	Gurvich1989	Spectroscopic determination of D_0(OH)
	9.8	Pople1985	MP4/6-311+G(2df,p)//UHF/6-31G(d)
	[9.26±0.29]	Barrow1956	measurement of D_0(OH, $A^2\Sigma^+$); quoted in Ruscic2001
	8.97±0.35		(average of all 298 K values; except the MP4 value of Pople1985)
BrOO	*28.9±1.5*	*Grant2010*	*RCCSD(T)/CBS(Q5)+CV+SR+SO; quoted in Sandar2011-JPL*
	26±1	Pacios1999	CCSD(T)/AREP/TZ(2df)//UMP2/AREP/TZ(2df); quoted in Grant2010
	[28±1]	As above	
	26.0±9.6	JANAF1996	Based on a trend analysis of $\Delta_f H_0°$(OClO)/$D_0°$(ClO) and the accepted value of $D_0°$(BrO); quoted in Burcat2010 and Sandar2003-JPL from JANAF1996.
	[27.8±9.6]	As above	
	27.0±1.9		(average of all 298 K values)
OBrO	*40.6±1.5*	*Grant2010*	*RCCSD(T)/CBS(Q5)+CV+SR+SO; also in Sandar2010*
	39.2±1.7	Lee2004	CCSD(T, Full)/6-311+G(3d,f)
	39.2±1.1	Klemm2001	From appearance energy of BrO^+ from OBrO; quoted in Sandar2010-JPL
	[41.4±1.0]	As above	
	[39.6±1.9]	Klemm2001	Corrected G2 value of Alcami1998 (spin-orbit contribution for BrO).
	38.9±1.9	Klemm2001	Corrected CCSD(T) value of ref. 19 (spin-orbit contribution for BrO).
	[39.4±1.9]	Klemm2001	As above
	30±3	Pacios1999	CCSD(T)/AREP/TZ(2df)//UMP2/AREP/TZ(2df); quoted in Grant2010
	[32±3]	As above	
	[37.5]	Alcami1998	G2; quoted in Klemm2001
	34.4±3	Workman1998	CCSD(T)/6-311+G(3df)//CCSD(T)/6-311G(2df); quoted in Klemm2001
	[34.5±3]	As above	
	36.3±6.0	JANAF1996	Quoted in Burcat2010 from JANAF1996.
	39.2±1.1	JANAF1996	Quoted in Sandar2003-JPL from JANAF1996.
	[38.6±6]	JANAF1996	Based on a trend analysis of $\Delta_f H_0°$(OClO)/$D_0°$(ClO) and the accepted value of $D_0°$(BrO); quoted in Klemm2001
	[31.55]	Huie1995	Quoted in Klemm2001; estimated from $\Delta G(BrO_2(aq))$
	[20.79]	Cottrell1954	Quoted in Klemm2001; derived from D(O-BrO)

	39.4±1.2		(average of all 298 K values, except the values of JANAF1996 (the lower value of 36.3), Pacios1999 & Workman1998)
ΔH_{298K}^{RX} (channel 1(a))	-47.5±2.1		using the averaged $\Delta H_{f,298K}$ values
	-47.7±1.1		using the best theoretical $\Delta H_{f,298K}$ values
	-47.7		{present study; UCCSD(T)/CBS + SO(BrO)}
	-47.5		{present study; BD(TQ)/CBS + SO(BrO)}
ΔH_{298K}^{RX} (channel 1(b))	-25.0±2.1		using $\Delta H_{f,298}$ of O_2 $a^1\Delta_g$ =22.5 kcal.mol^{-1} from JPL 10-6
	-25.2±1.5		using the best theoretical $\Delta H_{f,298K}$ values
	-25.0		{present study; BD(TQ)/CBS + SO(BrO)}
ΔH_{298K}^{RX} (channel 2)	-7.1±3.3		using the averaged $\Delta H_{f,298K}$ values
	-4.2(>±0.5)		using the best theoretical $\Delta H_{f,298K}$ values
	-4.3		{present study; BD(TQ)/CBS + SO(BrO)}
ΔH_{298K}^{RX} (channel 3)	15.3±2.8		using the averaged $\Delta H_{f,298K}$ values
	17.1±2.0		using the best theoretical $\Delta H_{f,298K}$ values
	14.9		{present study; BD(TQ)/CBS + SO(BrO)}
ΔH_{298K}^{RX} (channel 4)	2.9±3.5		using the averaged $\Delta H_{f,298K}$ values
	5.4±2.0		using the best theoretical $\Delta H_{f,298K}$ values
	5.9		{present study; BD(TQ)/CBS + SO(BrO)}

For BrO, the ground electronic state is $X^2\Pi$, and the experimental equilibrium spin-orbit (SO) state separation between the $X_2{}^2\Pi_{1/2}$ and $X_1{}^2\Pi_{3/2}$ states is 975.43 cm^{-1} (or 2.7889 kcal.mol^{-1}) [B. J. Drouin, C. E. Miller, H. S. P. Muller, E. A. Cohen, *J. Mol.Spectrosc.* 2001, **205**, 128.]. Using this SO splitting, the $X_2{}^2\Pi_{3/2}$ SO state of BrO should be lower than the unperturbed $X^2\Pi$ state by 1.3944 kcal.mol^{-1}. This reduces the computed ΔH_{298K}^{RX} value by the same amount.

Alcami1998: Alcami, M. and Cooper, I. L. *Ab initio* calculations on bromine oxide and dioxides and their corresponding anions. J. Chem. Phys. 1998, 108, 9414.

Aran1997: Aranda, A.; LeBras, G.; LaVerdet, G.; Poulet, G. The BrO + CH_3O_2 Reaction: Kinetics and Role in the Atmospheric Ozone Budget. Geophys. Res. Lett. 1997, 24, 2745−2748.

ATcT2014: Active Thermochemical Tables, http://atct.anl.gov/ (accessed October 13, 2014).

Barrow1956: Barrow, R. F. Ark. Fys. 1956, 11, 281.

Bed1997: Bedjanian, Y.; LeBras, G.; Poulet, G. Kinetic Study of the Br+IO, I+BrO and Br+I_2 Reactions. Heat of Formation of the BrO Radical. Chem. Phys. Lett. 1997, 266, 233−238.

Burcat2010: A. Burcat, B. Ruscic, Third Millennium Ideal Gas and Condensed Phase Thermochemical Database for Combustion with Updates from Active Thermochemical Tables,

Chemistry Division, Argonne National Laboratory, Argonne, Illinois, September 2005, (last update: March 15, 2010); this database is available in electronic form at: ftp://ftp.technion.ac.il/pub/supported/aetdd/thermodynamics.

Canneaux2012: Canneaux, S.; Hammaecher, C.; Cours, T.; Louis, F. and Ribaucour, M. Theoretical Study of H-Abstraction Reactions from CH_3Cl and CH_3Br Molecules by ClO and BrO Radicals. J. Phys. Chem. A 2012, 116, 4396−4408.

Cottrell1954: Cottrell, T. L.The Strength of Chemical Bonds; Butterworth: London, 1954; P.221-81.

Cox1989: Cox, J. D., D. D. Wagman and V. A. Medvedev CODATA Key Values for Thermodynamics; Hemisphere Publishing Corp.: New York, 1989.

Csaszar2010: Csaszar, A.G. and Furtenbacher, T. From a Network of Computed Reaction Enthalpies to Atom-Based Thermochemistry (NEAT). Chem. Eur. J. 2010, 16, 4826 – 4835.

DeM1994: DeMore, W.B.; Sander, S.P.; Golden, D.M. ; Hampson, R.F.; Kurylo, M.J.; Howard, C.J.; Ravishankara, A.R.; Kolb, C.E. and Molina, M. Chemical kinetics and Photochemical Data for Use in Stratospheric Modeling, Jet Propulsion Lab., Pasadena, CA, 1994, JPL Publ. 94-26.

Den2004: Denis, P. A. On the Performance of CCSD(T) and CCSDT in the Study of Molecules with Multiconfigurational Character: Halogen Oxides, HSO, BN and O_3. Chem. Phys. Lett. 2004, 395, 12−20.

Den2006: Denis, P. A. Thermochemistry of the Hypobromous and Hypochlorous Acids, HOBr and HOCl. J. Phys. Chem. A 2006, 110, 5887−5892.

Esp1993: Espinosa-Garcia, J. New theoretical value of the enthalpy of formation of the OOH radical. Mol. Phys. 1993, 79, 445-447.

Esp1999: Espinosa-Garcia, J. Theoretical Enthalpies of Formation of RO_x (R = H, CH_3; X = F, Cl, Br) Compounds. Chem. Phys. Lett. 1999, 315, 239−247.

Fan2005: Fabian, W. M. F.; Kalcher, J. and Janoschek, R. Stationary points on the energy hypersurface of the reaction $O_3 + H\bullet \rightarrow [\bullet O_3H]^* \leftrightarrows O_2 + \bullet OH$ and thermodynamic functions of $\bullet O_3H$ at G3MP2B3, CCSD(T)-CBS (W1U) and MR-ACPF-CBS levels of theory. Theor. Chem. Acc. 2005, 114, 182-188.

Feller2003: Feller, D.; Peterson, K.A.; de John, W.A. and Dixon, D.A. Performance of coupled cluster theory in thermochemical calculations of small halogenated compounds. J. Chem. Phys. 2003, 118, 3510.

Feller2008: Feller, D.; Peterson, K.; Dixon, D. A Survey of Factors Contributing to Accurate Theoretical Predictions of Atomization Energies and Molecular Structures. J. Chem. Phys. 2008,129, 204105.

Flowers2004: Flowers, B. A.; Szalay, P. G.; Vazquéz, J.; Stanton, J. F.; Kállay, M.; Gauss, J.; Császár, A. G. Benchmark Thermochemistry of the Hydroperoxyl Radical. J. Phys. Chem. A

2004,108, 3195−3199.
Ganyecz2015: Ganyecz, Á.; Csontos, J.; Nagy, B. and Kállay, M. Theoretical and Thermochemical Network Approaches To Determine the Heats of Formation for HO_2 and Its Ionic Counterparts. J. Phys. Chem. A 2015,119,1164-1176.
Gold2012: Goldsmith, C.F.; Magoon, G.R. and Green, W.H. Database of Small Molecule Thermochemistry for Combustion. J. Phys. Chem. A 2012, 116, 9033−9057.
Grant2009: Grant, D. J .; Dixon, D. A .; Francisco, J. S .; Feller, D .; Peterson, K. A . Heats of Formation of the $H_{1,2}O_mS_n$ (m, n = 0−3) Molecules from Electronic Structure Calculations. J. Phys. Chem. A 2009,113, 11343–11353.
Grant2010: Grant, D. J. ; Garner III, E. B.; Matus, M. H.; Nguyen, M. T.; Peterson, K. A.; Francisco, J. S. and Dixon, D. A. Thermodynamic Properties of the XO_2, X_2O, XYO, X_2O_2, and XYO_2 (X, Y = Cl, Br, and I) Isomers. J. Phys. Chem. A 2010, 114, 4254–4265.
Guha1999: Guha, S. and Francisco, J.S. An Examination of the Reaction Pathways for the HOOOBr and HOOBrO Complexes Formed from the HO2 + BrO Reaction. J. Phys. Chem. A 1999, 103, 8000-8007.
Gurvich1989: Gurvich, L. V.; Veyts, I. V.; Alcock, C. B. Thermodynamic Properties of Individual Substances; Hemisphere: New York, 1989; Vol. 1.
Gurvich1991: Gurvich, L. V., I. V. Veyts and C. B. Alcock Thermodynamic Properties of Individual Substances,, Fourth ed.; Hemisphere Publishing Corp.: New York, 1991; Vol. 2.
Harding2008: Active Thermochemical Tables (ATcT) using the Core (Argonne) Thermochemical Network Version 1.064. Harding, M. E.; Va´zquez, J.; Ruscic, B.; Wilson, A. K.; Gauss, J.; Stanton, J. F. *J. Chem. Phys.* **2008**, *128*, 114111. Ruscic, B.; Pinzon, R. E.; Morton, M. L.; Laszewski, G. v.; Bittner, S.; Nijsure, S. G.; Amin, K. A.; Minkoff, M.; Wagner, A. F. *J. Phys. Chem. A* **2004**, *108*, 9979. Ruscic, B.; Pinzon, R. E.; Laszewski, G. v.; Kodeboyina, D.; Burcat, A.; Leahy, D.; Montoya, D.; Wagner, A. F. *J. Phys. Conf. Ser.* **2005**, *16*, 561. Ruscic, B.; Pinzon, R. E.; Morton, M. L.; Srinivasan, N. K.; Su, M.-C.; Sutherland, J. W.; Michael, J. V. *J. Phys. Chem. A* **2006**, *110*, 6592.
Has1997: Hassanzadeh, P. and Irikura, K. K. Nearly *ab Initio* Thermochemistry: The Use of Reaction Schemes. Application to IO and HOI. J. Phys. Chem. A 1997,101,1580.
Haw2002: Haworth, N.L. and Bacskay, G.B. Heats of formation of phosphorus compounds determined by current methods of computational quantum chemistry. J. Chem. Phys. 2002, 117, 11175.
Henry2002: Henry, D.J.; Parkinson, C.J. and Radom, L. J. Phys. Chem. A 2002, 106, 7927-7936.
Herbon2002: Herbon, J.T.; Hanson, R.K.; Golden, D. M. and Bowman, C. T. Proceedings of the Combustion Institute, 2002, 29, 1201–1208.
Hill1984: Hills, A.J. and Howard, C.J. Rate coefficient temperature dependence and branching ratio for the OH+ClO reaction. J. Chem. Phys. 1984, 81, 4458. http://dx.doi.org/10.1063/1.447414.
Huber1998: Constants of Diatomic Molecules; Huber, K. P. and G. Herzberg, Eds.; National

Institute of Standards and Technology, 1998.
Huie1995: Huie, R. E.; Laszlo, B. The Atmospheric Chemistry of Iodine Compounds. In Halon Replacements: Technology and Science; ACS Symposium Series 611; American Chemical Society: Washington, DC,1995; p 31.
JANAF1994: Chase, M. W.; Davies, C. A.; Downey, J. R.; Frurip, D. J.; McDonald, R. A.; Syverud, A. N. J. Phys. Chem. Ref. Data Suppl.1985, 1.
JANAF1996: Chase, M. W., "NIST-JANAF Thermochemical Tables for the Bromine Oxide," J. Phys. Chem. Ref. Data 1996, 25, 1069-1111.
JANAF1998: Chase, M. W., Jr. NIST-JANAF Thermochemical Tables, 4th ed.; J. Phys. Chem. Ref. Data, Monograph 1998, 9.
Joe2001: Joens, J. A. The Dissociation Energy of OH($X^2\Pi_{3/2}$) and the Enthalpy of Formation of OH($X^2\Pi_{3/2}$), ClOH, and BrOH from Thermochemical Cycles. J. Phys. Chem. A 2001, 105, 11041−11044.
Jur1999: Jursic, B. S. High Level *Ab Initio* and Density Functional Theory Study of Bond Dissociation Energy and Enthalpy of Formation for Hypochloric and Hypobromic Acids. J. Mol. Struct.: THEOCHEM 1999, 467, 173−179.
Karton2009: Karton, A.; Parthiban, S. and Martin, J.M.L. Post-CCSD(T) *ab Initio* Thermochemistry of Halogen Oxides and Related Hydrides XOX, XOOX, HOX, XO_n, and HXO_n (X = F, Cl), and Evaluation of DFT Methods for These Systems. J. Phys. Chem. A 2009, 113, 4802–4816.
Karton2011: Karton, A.; Daon, S.; Martin, J. M. L. W4-11: A high-confidence benchmark dataset for computational thermochemistry derived from first-principles W4 data. Chem. Phys. Letters, 510 (2011) 165–178.
Kim2006: Kim, H., Dooley, J. S.; Johnson, E. R. and North, S. W. Photodissociation of the BrO radical using velocity map ion imaging: Excited state dynamics and accurate D_0^0(BrO) evaluation. J. Chem. Phys. 2006, **124**, 134304.
Klemm2001: Klemm, R. B.; Thorn, R.P.; Stief, L.J.; Buckley, T.J. and Johnson, R.D. Heat of Formation of OBrO: Experimental Photoionization Study. J. Phys. Chem. A 2001, 105, 1638-1642.
Lee2004: Lee, S.Y. Computational Study of Enthalpies of Formation of OXO (X = Cl, Br, and I) and Their Anions. J. Phys. Chem. A, 2004, 108, 10754-10761.
Litorja1998: Litorja, M.; Ruscic, B. A Photoionization Study of the Hydroperoxyl Radical, HO_2, and Hydrogen Peroxide, H_2O_2. J. Electron Spectrosc. Relat. Phenom. 1998, 97, 131−146.
Loc1996: Lock, M.; Barnes, R. J.; Sinha, A. Near-Threshold Photodissociation Dynamics of Hobr: Determination of Product State Distribution, Vector Correlation, and Heat of Formation. J. Phys. Chem. 1996, 100, 7972−7980.
McG1994: McGrath, M.P. and Rowland, F.S. J. Phys. Chem. 1994, 98, 4773.
Mes1999: Messer, B. M.; Elrod, M. J.; Theoretical, A. Study of ROx (R = H, CH_3; X = F, Cl, Br)

Enthalpies of Formation, Ionization Potentials and Fluoride Affinities. Chem. Phys. Lett. 1999, 301, 10−18.
Mor2012: Morgon, N.H. Enthalpies of Formation of Phosphorus and Oxygen Compounds Determined by the Correlation Consistent Composite Approach. Int. J. Quantum Chemistry 2012, 112, 3256–3260.
Orl1996: Orlando, J. J.; Tyndall, G. S. Rate Coefficients for the Thermal Decomposition of $BrONO_2$ and the Heat of Formation of $BrONO_2$. J. Phys. Chem. 1996, 100, 19398−19405.
Orn2007: Ornellas, F. R. Thermochemistry of New Molecular Species: SBr and HSBr. J. Chem. Phys. 2007, 126,204314; DOI: 10.1063/1.2737776.
Pacios1999: Pacios, L.F. and Geomez, P.C. Bonding in bromine oxides: Isomers of BrO_2, Br_2O_2 and BrO_3. J. Mol. Struct. (Theochem) 1999, 467, 223-231.
Pasadena, California, February 1, 2003, http://jpldataeval.jpl.nasa.gov/.
Peterson2006: Peterson, K. A.; Shepler, B. C.; Figgen, D.; Stoll, H. On the Spectroscopic and Thermochemical Properties of ClO, BrO, IO, and Their Anions. J. Phys. Chem. A 2006, 110, 13877−13883.
Pople1985: Pople, J.A.; Luke, B.T.; Frisch, M.J. and Binkley, J.S. Theoretical Thermochemistry. 1. Heats of Formation of Neutral AH, Molecules (A = Li to CI). J. Phys. Chem. 1985, 89, 2198-2203.
Ramond2002: Ramond, T.; Blanksby, S.; Kato, S.; Bierbaum, V.; Davico, G.; Schwartz, R.; Lineberger, W.; Ellison, G. Heat of Formation of the Hydroperoxyl Radical HOO Via Negative Ion Studies. J. Phys. Chem. A 2002, 106, 9641−9647.
Rus1994: Ruscic, B.; Berkowitz, J. Experimental determination of ΔH^0_f(HOBr) and ionization potentials (HOBr): Implications for corresponding properties of HOI. J. Chem. Phys. 1994, 101, 7795-7803.
Ruscic2001: Ruscic, B.; Feller, D.; Dixon, D.A.; Peterson, K.A.; Harding, L.B.; Asher, R.L. and Wagner, A.F. Evidence for a Lower Enthalpy of Formation of Hydroxyl Radical and a Lower Gas-Phase Bond Dissociation Energy of Water. J. Phys. Chem A 2001, 105, 1-4.
Ruscic2002: Ruscic, B.; Wagner, A.F.; Harding, L.B.; Asher, R.L.; Feller, D.; Dixon, D.A.; Peterson, K.A.; Song, Y.; Qian, X.; Ng, C-Y.; Liu, J.; Chen, W. and Schwenke, D.W. On the Enthalpy of Formation of Hydroxyl Radical and Gas-Phase Bond Dissociation Energies of Water and Hydroxyl. J. Phys. Chem. A 2002, 106, 2727-2747.
Ruscic2004: Ruscic, B.; Pinzon, R.E.; Morton, M.L.; von Laszevski, G.; Bittner, S.J.; Nijsure, S.G.; Amin, K. A.; Minkoff, M. and Wagner, A.F. Introduction to Active Thermochemical Tables: Several "Key" Enthalpies of Formation Revisited. J. Phys. Chem. A, 2004,108, 9979-9997.
Ruscic2006 ATcT: Ruscic, B.; Pinzon, R. E.; Morton, M. L.; Srinivasan, N. K.; Su, M.-C.; Sutherland, J. W.; Michael, J. V. Active Thermochemical Tables: Accurate Enthalpy of Formation of Hydroperoxyl Radical, HO_2. J. Phys. Chem. A 2006,110, 6592-6601.

Ruscic2011: Ruscic, B. Active Thermochemical Tables: version Alpha 1.110 of the Core (Argonne) Thermochemical Network, release date 04.02.2011.
Ruscic2014: Ruscic, B.; Feller, D.; Peterson, K. A. Active Thermochemical Tables: Dissociation Energies of Several Homonuclear First-Row Diatomics and Related Thermochemical Values. Theor. Chem. Acc. 2014, 133, 1415/1−12.
Ruscic2015: Ruscic, B. Active Thermochemical Tables: Sequential Bond Dissociation Enthalpies of Methane, Ethane, and Methanol and the Related Thermochemistry. J. Phys. Chem. A 2015,119,7810−7837.
San2001: Santos, C. M. P.; Faria, R. B.; Machuca-Herrera, J. O.; Machado, S. D. Equilibrium Geometry, Vibrational Frequencies, and Heat of Formation of HOBr, $HBrO_2$, and $HBrO_3$ Isomers. Can. J. Chem.-Rev. Can. Chim. 2001, 79, 1135−1144.
Sandar2003-JPL: S. P. Sander, R. R. Friedl, D. M. Golden, M. J. Kurylo, R. E. Huie, V. L. Orkin, G. K. Moortgat, A. R. Ravishankara, C. E. Kolb, M. J. Molina and B. J.Finlayson-Pitts, JPL Publication 02-25, Chemical Kinetics and Photochemical Data for Use in Atmospheric Studies, Evaluation Number 14, National Aeronautics and Space Administration, Jet Propulsion Laboratory, California Institute of Technology
Sander2011: Sander, S. P., J. Abbatt, J. R. Barker, J. B. Burkholder, R. R. Friedl, D. M. Golden, R. E. Huie, C. E. Kolb, M. J. Kurylo, G. K. Moortgat, V. L. Orkin and P. H. Wine "Chemical Kinetics and Photochemical Data for Use in Atmospheric Studies, Evaluation No. 17," JPL Publication 10-6, Jet Propulsion Laboratory, California Institute of Technology**,** Pasadena, 2011.
Shum1983: Shum, L.; Benson, S. Review of the Heat of Formation of the Hydroperoxyl Radical. J. Phys. Chem. 1983, 87, 3479−3482.
Silva2011: da Silva, G. Kinetics and Mechanism of the Glyoxal + HO_2 Reaction: Conversion of HO_2 to OH by Carbonyls. J. Phys. Chem. A 2011,115, 291-297.
Tajti2004: Tajti, A.; Szalay, P. G.; Csaszar, A. G.; Kállay, M.; Gauss, J.; Valeev, E. F.; Flowers, B. A.; Vázquez, J. and Stanton, J. F. HEAT: High accuracy extrapolated *ab initio* thermochemistry. J. Chem. Phys. 2004,121, 11599 – 11613.
Tan1999: Taniguchi, N.; Takahashi, K.; Matsumi, Y.; Dylewski, S.M.; Geiser, J.D. and Houston, P.L. Determination of the heat of formation of O_3 using vacuum ultraviolet laser-induced fluorescence spectroscopy and two-dimensional product imaging techniques. J. Chem. Phys. 1999, 111 , 6350
Wie1992: Wiedmann, R.T.; Tonkyn, R.G. and White, M.G. Rotationally resolved threshold photoelectron spectra of OH and OD. J. Chem. Phys. 1992, 97, 768.
Wil1999: Wilmouth, D. M.; Hanisco, T. F.; Donahue, N. M.; Anderson, J. G. Fourier Transform Ultraviolet Spectroscopy of the a $A\ ^2\Pi_{3/2} \leftarrow X^2\Pi_{3/2}$ Transition of BrO. J. Phys. Chem. A 1999, 103, 8935−8945.
Workman1998: Workman, M.A. and Francisco, J.S. Molecular structure and energetics of BrO_x radicals (where x =1, 2, and 3). Chemical Physics Letters 1998,293, 65–71.

Table S2. Computed spin densities with unrestricted wavefunctions of all atoms in the transition state of channel 1(b) BrO + HO_2 → HOBr + O_2 ($\tilde{a}^1\Delta_g$) (see text).

Atom	Levels of theory					
	M06-2X/ AVDZ	BD/AVDZ	BD(T)/AVTZ// M06-2X/AVDZ	BD(T)/AVTZ// BD/AVDZ	BD(T)/AVQZ// M06-2X/AVDZ	BD(T)/AVQZ// BD/AVDZ
Br	0.365983	0.337768	0.370982	0.000000	0.368173	0.000000
O	0.525253	0.404465	0.565513	0.000000	0.569491	0.000000
H	-0.011192	-0.026403	-0.015772	0.000000	-0.011449	0.000000
O	-0.273028	-0.220575	-0.242201	0.000000	-0.255235	0.000000
O	-0.607017	-0.495256	-0.678522	0.000000	-0.670981	0.000000

Table S3. Computed (BD(TQ)/CBS//M06-2X/AVDZ incl. SO correction for BrO) k_{outer} , k_{inner} and $k_{overall}$ values in $cm^3.molecule^{-1}s^{-1}$ of channel 1(b) BrO + HO_2 → HOBr + O_2 ($\tilde{a}^1\Delta_g$) at 200 – 400 K. k_{outer}, k_{inner} were calculated from PST and E,J-TST respectively using VARIFLEX and $k_{overall(i)}$ was calculated using equation (1).

T (K)	k_{outer}	k_{inner}	$k_{overall(i)}$
200	2.49E-10	7.39E-11	5.70E-11
210	2.51E-10	5.23E-11	4.33E-11
220	2.52E-10	3.83E-11	3.33E-11
230	2.54E-10	2.89E-11	2.60E-11
240	2.55E-10	2.24E-11	2.06E-11
250	2.57E-10	1.78E-11	1.67E-11
260	2.58E-10	1.44E-11	1.37E-11
270	2.59E-10	1.19E-11	1.14E-11
280	2.6E-10	9.98E-12	9.61E-12
298	2.62E-10	7.53E-12	7.32E-12
300	2.63E-10	7.31E-12	7.12E-12
310	2.63E-10	6.37E-12	6.22E-12
320	2.64E-10	5.61E-12	5.50E-12
330	2.65E-10	4.99E-12	4.90E-12
340	2.66E-10	4.48E-12	4.40E-12
350	2.67E-10	4.04E-12	3.98E-12
360	2.67E-10	3.68E-12	3.63E-12
370	2.68E-10	3.37E-12	3.33E-12
380	2.68E-10	3.11E-12	3.07E-12
390	2.69E-10	2.88E-12	2.85E-12
400	2.69E-10	2.68E-12	2.65E-12

Table S4. Computed (BD(TQ)/CBS//M06-2X/AVDZ incl. SO correction for BrO) k_{inner} values calculated with the E,J-TST (with VARIFLEX) and TST (with POLYRATE) methods in $cm^3.molecule^{-1}s^{-1}$ for channel 1(b) BrO + HO_2 → HOBr + O_2 ($\tilde{a}^1\Delta_g$) at 200 – 400 K. [(a)]

T (K)	E,J-TST	TST [(b)]
200	7.39E-11	6.65E-11 (7.04E-11)
210	5.23E-11	4.69E-11
220	3.83E-11	3.43E-11
230	2.89E-11	2.59E-11
240	2.24E-11	2.00E-11
250	1.78E-11	1.59E-11
260	1.44E-11	1.28E-11
270	1.19E-11	1.06E-11
280	9.98E-12	8.86E-12
298	7.53E-12	6.67E-12 (6.93E-12)
300	7.31E-12	6.48E-12
310	6.37E-12	5.64E-12
320	5.61E-12	4.96E-12
330	4.99E-12	4.41E-12
340	4.48E-12	3.95E-12
350	4.04E-12	3.57E-12
360	3.68E-12	3.25E-12
370	3.37E-12	2.97E-12
380	3.11E-12	2.74E-12
390	2.88E-12	2.54E-12
400	2.68E-12	2.36E-12 (2.43E-12)

(a) ΔZPE is included in the barrier height (of -3.07 $kcal.mol^{-1}$) used in the VARIFLEX (E,J-TST) calculations (column 2) but not in the POLYRATE (TST) calculations (column 3), which use the classical barrier height (-3.05 $kcal.mol^{-1}$).

(b) Values shown in brackets at 200, 298 and 400 K (in column 3) are from conventional TST calculations (with POLYRATE) with a barrier height (-3.07 $kcal.mol^{-1}$) which is -3.05 $kcal.mol^{-1}$ plus the ΔZPE contribution. These results show that the difference between the E,J-TST and TST results shown in the table arises from (i) a difference in the barrier height used as well as (ii) the microcanonical treatment of the reactants and TS in the E,J-TST method compared to a Boltzmann distribution in the reactants and TS used in the conventional TST method.

Table S5. Computed (BD(TQ)/CBS//M06-2X/AVDZ incl. SO correction for BrO) values of k_{inner} at various VTST levels (TST, CVT and ICVT) with and without CAG correction in $cm^3.molecule^{-1}s^{-1}$ for channel 1(b) $BrO + HO_2 \rightarrow HOBr + O_2\,(\tilde{a}^1\Delta_g)$ at 200 – 400 K, calculated with POLYRATE.

T (K)	TST	TST/CAG	CVT	CVT/CAG	ICVT
200	6.645E-11	7.4903E-12	8.462E-12	8.0651E-12	8.4618E-12
210	4.69E-11	5.8658E-12	6.5949E-12	6.298E-12	6.5947E-12
220	3.4291E-11	4.7138E-12	5.2752E-12	5.0468E-12	5.2751E-12
230	2.585E-11	3.8737E-12	4.316E-12	4.1358E-12	4.3159E-12
240	2.0014E-11	3.246E-12	3.6014E-12	3.4561E-12	3.6013E-12
250	1.5863E-11	2.7669E-12	3.0573E-12	2.938E-12	3.0573E-12
260	1.2834E-11	2.3942E-12	2.6352E-12	2.5355E-12	2.6352E-12
270	1.0575E-11	2.0993E-12	2.3021E-12	2.2175E-12	2.3021E-12
280	8.8565E-12	1.8626E-12	2.0352E-12	1.9625E-12	2.0352E-12
298	6.6681E-12	1.5409E-12	1.6733E-12	1.6164E-12	1.6733E-12
300	6.4773E-12	1.5115E-12	1.6404E-12	1.5848E-12	1.6404E-12
310	5.6408E-12	1.3795E-12	1.4924E-12	1.4431E-12	1.4924E-12
320	4.964E-12	1.2686E-12	1.3682E-12	1.3241E-12	1.3682E-12
330	4.4102E-12	1.1747E-12	1.2632E-12	1.2233E-12	1.2631E-12
340	3.952E-12	1.0944E-12	1.1735E-12	1.1372E-12	1.1735E-12
350	3.5692E-12	1.0253E-12	1.096E-12	9.9334E-13	1.0959E-12
360	3.2465E-12	9.6549E-13	1.0274E-12	9.3369E-13	1.0274E-12
370	2.9722E-12	9.1339E-13	9.6789E-13	8.8174E-13	9.6785E-13
380	2.7374E-12	8.6777E-13	9.1583E-13	8.3627E-13	9.158E-13
390	2.535E-12	8.2762E-13	8.7008E-13	7.9627E-13	8.7005E-13
400	2.3594E-12	7.9214E-13	8.297E-13	7.6092E-13	8.2967E-13

Table S6.

Computed (BD(TQ)/CBS//M06-2X/AVDZ incl. SO correction for BrO) values of k_{inner} at various VTST levels (TST, CVT and ICVT) with tunneling correction at the Wigner, ZCT and SCT levels in $cm^3.molecule^{-1}s^{-1}$ for channel 1(b) $BrO + HO_2 \rightarrow HOBr + O_2(\tilde{a}^1\Delta_g)$ at 200 – 400 K calculated with POLYRATE.

T (K)	TST/W	TST/ZCT	CVT/ZCT	ICVT/ZCT	TST/SCT	CVT/SCT	ICVT/SCT
200	7.39E-11	7.49E-12	8.07E-12	8.46E-12	7.49E-12	8.07E-12	8.46E-12
210	5.17E-11	5.87E-12	6.30E-12	6.59E-12	5.87E-12	6.30E-12	6.59E-12
220	3.75E-11	4.71E-12	5.05E-12	5.28E-12	4.71E-12	5.05E-12	5.28E-12
230	2.81E-11	3.87E-12	4.14E-12	4.32E-12	3.87E-12	4.14E-12	4.32E-12
240	2.16E-11	3.25E-12	3.46E-12	3.60E-12	3.25E-12	3.46E-12	3.60E-12
250	1.70E-11	2.77E-12	2.94E-12	3.06E-12	2.77E-12	2.94E-12	3.06E-12
260	1.37E-11	2.39E-12	2.54E-12	2.64E-12	2.39E-12	2.54E-12	2.64E-12
270	1.12E-11	2.10E-12	2.22E-12	2.30E-12	2.10E-12	2.22E-12	2.30E-12
280	9.37E-12	1.86E-12	1.96E-12	2.04E-12	1.86E-12	1.96E-12	2.04E-12
298	7.01E-12	1.54E-12	1.62E-12	1.67E-12	1.54E-12	1.62E-12	1.67E-12
300	6.80E-12	1.51E-12	1.58E-12	1.64E-12	1.51E-12	1.58E-12	1.64E-12
310	5.91E-12	1.38E-12	1.44E-12	1.49E-12	1.38E-12	1.44E-12	1.49E-12
320	5.18E-12	1.27E-12	1.32E-12	1.37E-12	1.27E-12	1.32E-12	1.37E-12
330	4.59E-12	1.17E-12	1.22E-12	1.26E-12	1.17E-12	1.22E-12	1.26E-12
340	4.11E-12	1.09E-12	1.14E-12	1.17E-12	1.09E-12	1.14E-12	1.17E-12
350	3.70E-12	1.03E-12	9.93E-13	1.10E-12	1.03E-12	9.93E-13	1.10E-12
360	3.36E-12	9.65E-13	9.34E-13	1.03E-12	9.65E-13	9.34E-13	1.03E-12
370	3.07E-12	9.13E-13	8.82E-13	9.68E-13	9.13E-13	8.82E-13	9.68E-13
380	2.82E-12	8.68E-13	8.36E-13	9.16E-13	8.68E-13	8.36E-13	9.16E-13
390	2.61E-12	8.28E-13	7.96E-13	8.70E-13	8.28E-13	7.96E-13	8.70E-13
400	2.43E-12	7.92E-13	7.61E-13	8.30E-13	7.92E-13	7.61E-13	8.30E-13

Table S7. Computed (BD(TQ)/CBS//M06-2X/AVDZ incl. SO correction for BrO) $k_{overall(ii)}$ values obtained from k_{outer} and k_{inner} from equ.(1) for channel 1(b) BrO + HO_2 → HOBr + O_2 ($\tilde{a}^1\Delta_g$) at 200 – 400 K.

k_{outer} was obtained from PST calculations with VARIFLEX and k_{inner} was obtained from ICVT/SCT calculations with POLYRATE.

T (K)	k_{outer}	k_{inner}	$k_{overall(ii)}$
200	2.49E-10	8.46E-12	8.18E-12
210	2.51E-10	6.59E-12	6.42E-12
220	2.52E-10	5.28E-12	5.17E-12
230	2.54E-10	4.32E-12	4.25E-12
240	2.55E-10	3.60E-12	3.55E-12
250	2.57E-10	3.06E-12	3.02E-12
260	2.58E-10	2.64E-12	2.61E-12
270	2.59E-10	2.30E-12	2.28E-12
280	2.6E-10	2.04E-12	2.02E-12
298	2.62E-10	1.67E-12	1.66E-12
300	2.63E-10	1.64E-12	1.63E-12
310	2.63E-10	1.49E-12	1.48E-12
320	2.64E-10	1.37E-12	1.36E-12
330	2.65E-10	1.26E-12	1.25E-12
340	2.66E-10	1.17E-12	1.16E-12
350	2.67E-10	1.10E-12	1.10E-12
360	2.67E-10	1.03E-12	1.03E-12
370	2.68E-10	9.68E-13	9.65E-13
380	2.68E-10	9.16E-13	9.13E-13
390	2.69E-10	8.70E-13	8.67E-13
400	2.69E-10	8.30E-13	8.27E-13

Table S8.

A summary of values obtained for channel 1(b) BrO + HO_2 → HOBr + O_2 ($\tilde{a}^1\Delta_g$) using POLYRATE and employing the BD(TQ)/CBS//M06-2X/AVDZ (incl. SO correction for BrO) IRC (see text).

	BD(TQ)/CBS
$\Delta Ee^{\#}$ [a]	-3.05
$\Delta E_0^{\#}$ [a]	-3.07
s*(VaG)	-0.5516
VaG(s*) - VaG@s=0Å	0.8558
kCVT≈kICVT	Yes
κZCT=κSCT=1.0	Yes
κTST/CAG,200K	1.1219E-01
κCVT/CAG,200K	9.7397E-01
kTST,200K	6.6450E-11
kTST/CAG,200K	7.4550E-12
kCVT,200K	8.8185E-12
kICVT/SCT,200K	8.8184E-12
κTST/CAG,400K	3.3495E-01
κCVT/CAG,400K	9.1174E-01
kTST,400K	2.3594E-12
kTST/CAG,400K	7.9026E-13
kCVT,400K	8.3344E-13
kICVT/SCT,400K	8.3342E-13
ωi/cm^{-1}	228.51i
T/K with κTST/W≤1.2	200 K – 400 K

[a] Computed classical barrier height, $\Delta E_e^{\#}$ (electronic energy differences at s = 0, including spin-orbit contribution for BrO), and $\Delta E_0^{\#}$ (classical barrier height with zero-point correction, including spin-orbit contribution for BrO) in kcal.mol^{-1}. s*(V_a^G) is the position of the maximum of the V_aG curve (denoted as V_a^G(s*)) in Å. Computed rate coefficients, k's, are in $cm^3molecule^{-1}s^{-1}$.

Table S9. Computed (BQ(TQ)/CBS//M06-2X/AVDZ incl. SO correction for BrO) maximum change of Gibbs free energy of activation ($\Delta G^{\#}$) in kcal.mol^{-1} of channel 1(b) $BrO + HO_2 \rightarrow HOBr + O_2$ ($\tilde{a}^1\Delta_g$) along the reaction coordinate and corresponding location of s*(ΔG*) in Å from 200 K to 400 K from POLYRATE calculations.

T (K)	s*(ΔG*)	ΔG*
200	-0.495	21.6623
210	-0.495	22.8685
220	-0.405	24.076
230	-0.405	25.2839
240	-0.36	26.4912
250	-0.36	27.6988
260	-0.36	28.9062
270	-0.36	30.1129
280	-0.36	31.3192
298	-0.36	33.489
300	-0.36	33.73
310	-0.36	34.9347
320	-0.36	36.1388
330	-0.36	37.3425
340	-0.36	38.5456
350	-0.36	39.7484
360	-0.36	40.9506
370	-0.36	42.1524
380	-0.36	43.3538
390	-0.36	44.5548
400	-0.36	45.7553

Figures

Figure S1. Triplet reactant complex (RC), triplet transition state (TS) and triplet product complex (PC) of channel 1(a) BrO + HO_2 → HOBr + O_2 ($^3\Sigma_g^-$) at the M06-2X/AVDZ,AVDZ-PP level. Bond distances are shown Angstroms (Å).

Figure S2. Triplet transition states (TSs) of the channel 1(a) BrO + HO_2 → HOBr + O_2 ($^3\Sigma_g^-$) at the M06-2X/AVDZ, AVDZ-PP (upper) and BD/AVDZ,AVDZ-PP levels (lower). Bond distances are shown in Angstroms (Å).

Figure S3. Open-shell singlet reactant complex (RC), open-shell singlet transition state (TS), and closed-shell singlet product complex (PC) of channel 1(b) BrO + HO_2 → HOBr + O_2 ($\tilde{a}^1\Delta_g$) at the M06-2X/AVDZ,AVDZ-PP level. Bond distances are shown in Angstroms (Å).

Figure S4. Triplet transition states (TSs) of channel 1(b) BrO + HO_2 → HOBr + O_2 ($\tilde{a}^1\Delta_g$) at the M06-2X/AVDZ, AVDZ-PP (upper) and BD/AVDZ,AVDZ-PP levels (lower). Bond distances are shown in Angstroms (Å).

Figure S5. Open-shell singlet reactant complex (RC), open-shell singlet transition state (TS), and closed-shell singlet product complex (PC) of channel (2) BrO + HO_2 → HBr + O_3 at the M06-2X/AVDZ, AVDZ-PP level. Bond distances are shown in Angstroms (Å).

Figure S6. Separate reactants, triplet transition state (TS) and separate products of channel (4) BrO + HO_2 → BrOO + OH at the M06-2X/AVDZ, AVDZ-PP level. Bond distances are shown in Angstroms (Å).

Figure S7. Separate reactants, triplet transition state (TS) and separate products of channel (3) BrO

+ HO_2 → OBrO + OH at M06-2X/AVDZ, AVDZ-PP level. Bond distances are shown in Angstroms (Å).

Figure S8. Computed (BD(TQ)/CBS//M06-2X/CBS incl. SO correction for BrO) k_{outer}, k_{inner}, and $k_{overall(i)}$ ($cm^3molecule^{-1}s^{-1}$) versus T (K) curves of the channel 1(b) BrO + HO_2 → HOBr + O_2 ($\tilde{a}^1\Delta_g$). k_{outer} was evaluated at the PST level with VARIFLEX, k_{inner} was evaluated at the E,J-TST level with VARIFLEX and $k_{overall(i)}$ was calculated from k_{outer} and k_{inner} with equ.(1).

Figure S9. Computed k_{inner} (BD(TQ)/CBS//M06-2X/CBS incl. SO correction for BrO) values ($cm^3molecule^{-1}s^{-1}$) with TST for channel 1(b) BrO + HO_2 → HOBr + O_2 ($\tilde{a}^1\Delta_g$).

E,J-TST (with zero-point corrected barrier height) values were obtained with VARIFLEX and TST values (with the classical barrier height, which does not include zero-point correction) were obtained with POLYRATE.

Figure S10. Computed (BD(TQ)/CBS//M06-2X/CBS incl. SO correction for BrO) $k_{overall(ii)}$. ($cm^3molecule^{-1}s^{-1}$) versus T (K) curves for channel 1(b) BrO + HO_2 → HOBr + O_2 ($\tilde{a}^1\Delta_g$).

k_{outer} is evaluated with PST using VARIFLEX and k_{inner} is evaluated using ICVT/SCT with POLYRATE . $k_{overall(ii)}$ is obtained from k_{outer}, and k_{inner} , using equ.(1).

(The $k_{overall(ii)}$ values (blue triangles) are virtually superimposed on the k_{inner} values (red circles) in this figure).

Figure S1.

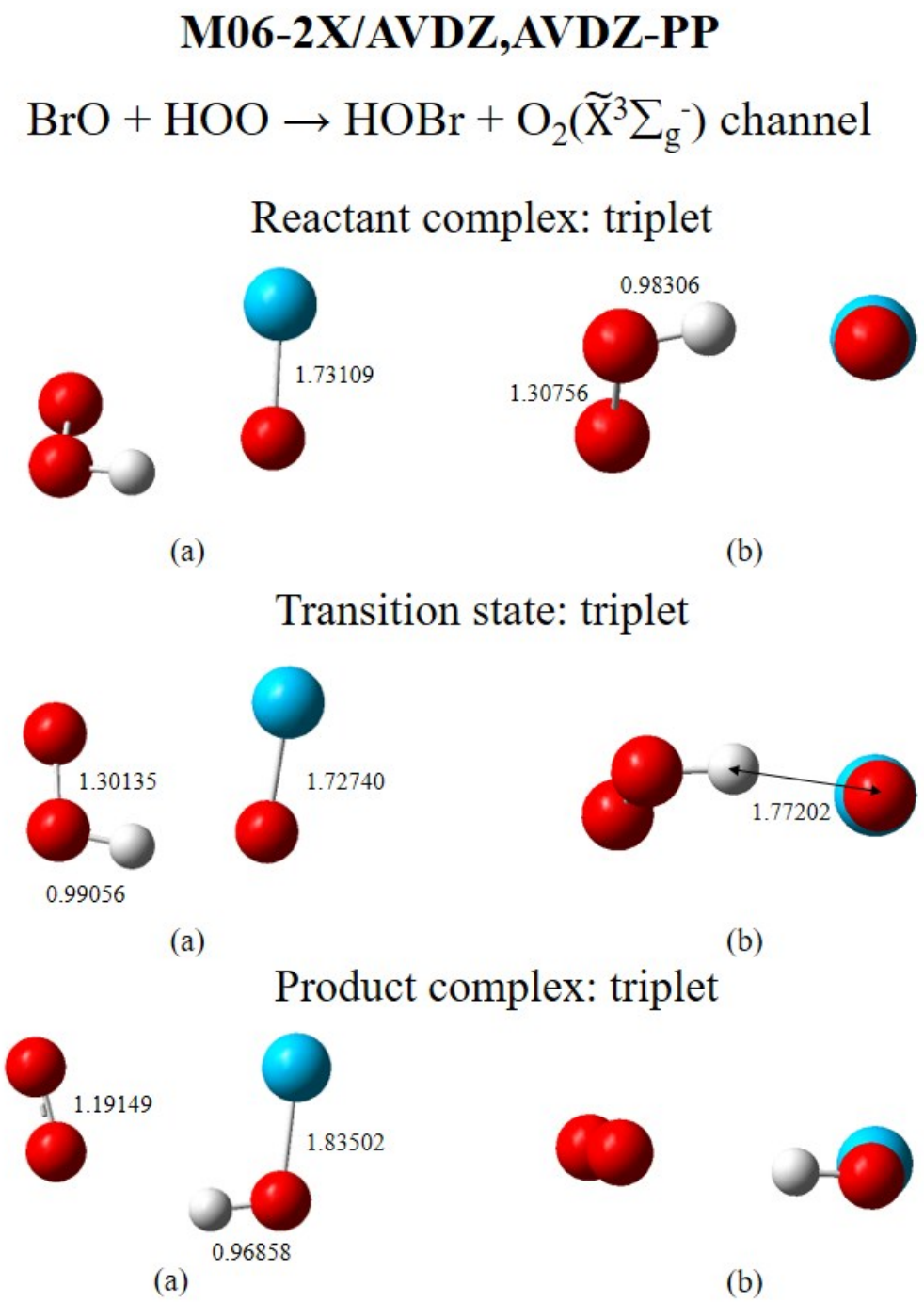
M06-2X/AVDZ,AVDZ-PP
BrO + HOO → HOBr + O2(X̃3Σg-) channel
Reactant complex: triplet
1.73109
0.98306
1.30756
(a)
(b)
Transition state: triplet
1.30135
1.72740
0.99056
1.77202
(a)
(b)
Product complex: triplet
1.19149
1.83502
0.96858
(a)
(b)

Figure S2.

Triplet Transition States

$BrO + HOO \rightarrow HOBr + O_2(\widetilde{X}^3\Sigma_g^-)$ channel

Transition state (M06-2X/AVDZ,AVDZ-PP)

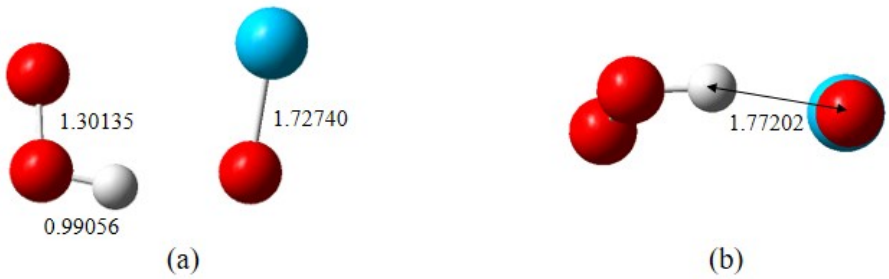

Transition state (BD/AVDZ,AVDZ-PP)

Figure S3.

M06-2X/AVDZ,AVDZ-PP

BrO + HOO → HOBr + $O_2(a^1\Delta_g)$ channel

Reactant complex: open-shell singlet

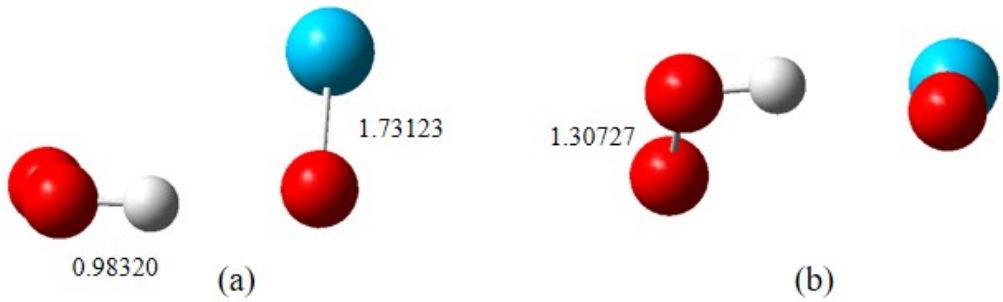

Transition state: open-shell singlet

Product complex: closed-shell singlet

Figure S4.

Singlet Transition States

BrO + HOO → HOBr + $O_2(\tilde{a}^1\Delta_g)$ channel

Transition state (M06-2X/AVDZ,AVDZ-PP)

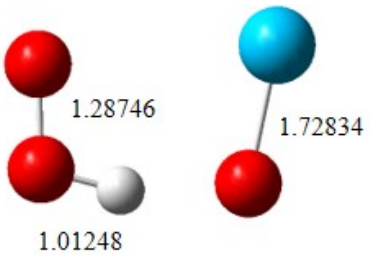

(a)

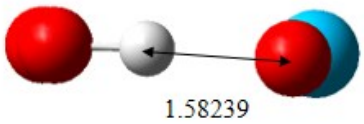

(b)

Transition state (BD/AVDZ,AVDZ-PP)

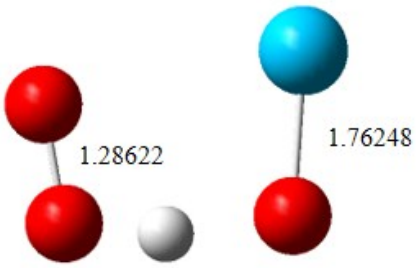

(a)

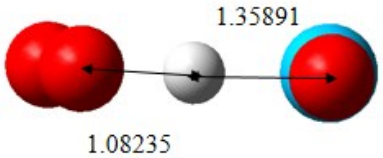

(b)

Figure S5.

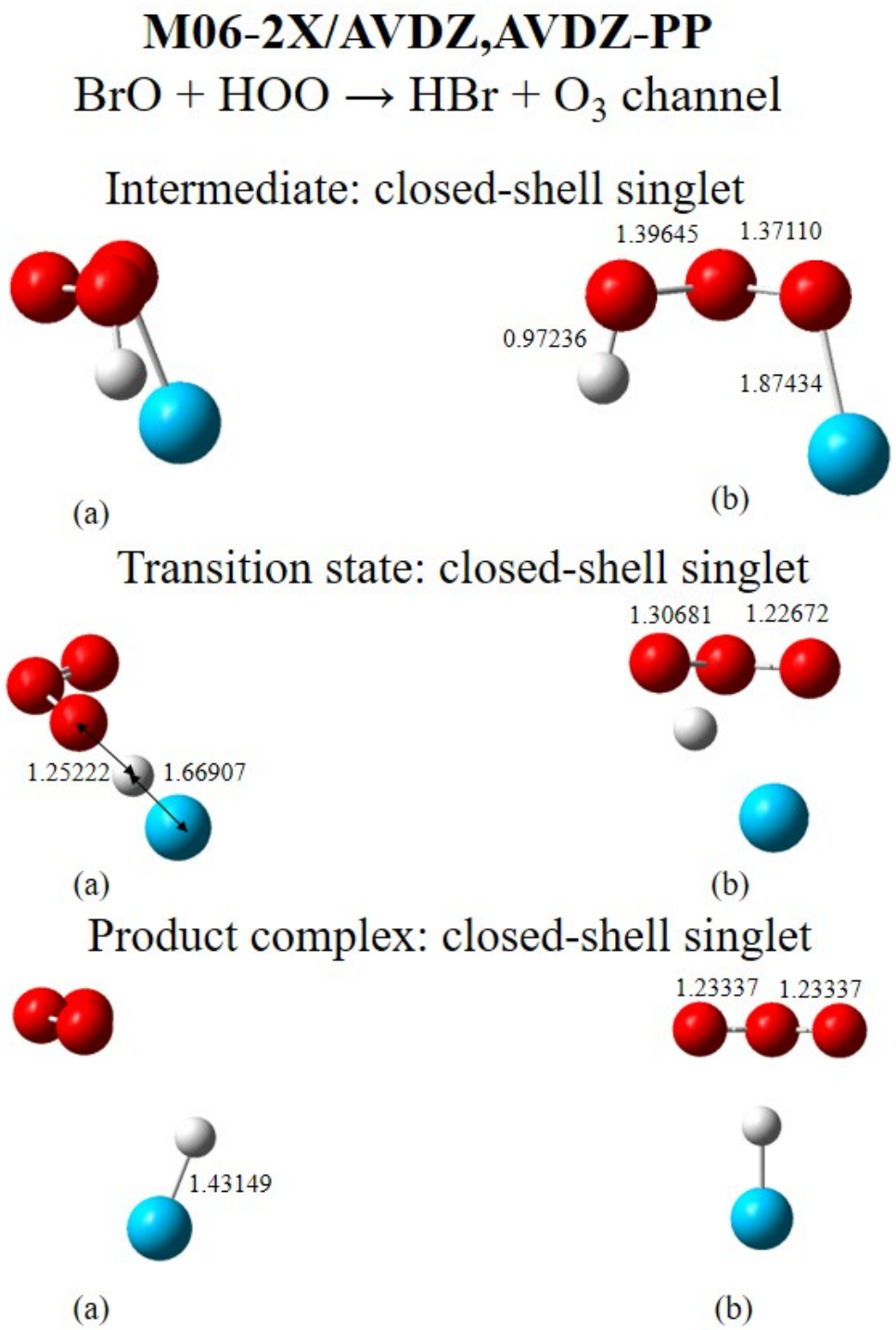
M06-2X/AVDZ,AVDZ-PP
BrO + HOO → HBr + O3 channel
Intermediate: closed-shell singlet
1.39645
1.37110
0.97236
1.87434
(a)
(b)
Transition state: closed-shell singlet
1.30681
1.22672
1.25222
1.66907
(a)
(b)
Product complex: closed-shell singlet
1.23337
1.23337
1.43149
(a)
(b)

Figure S6.

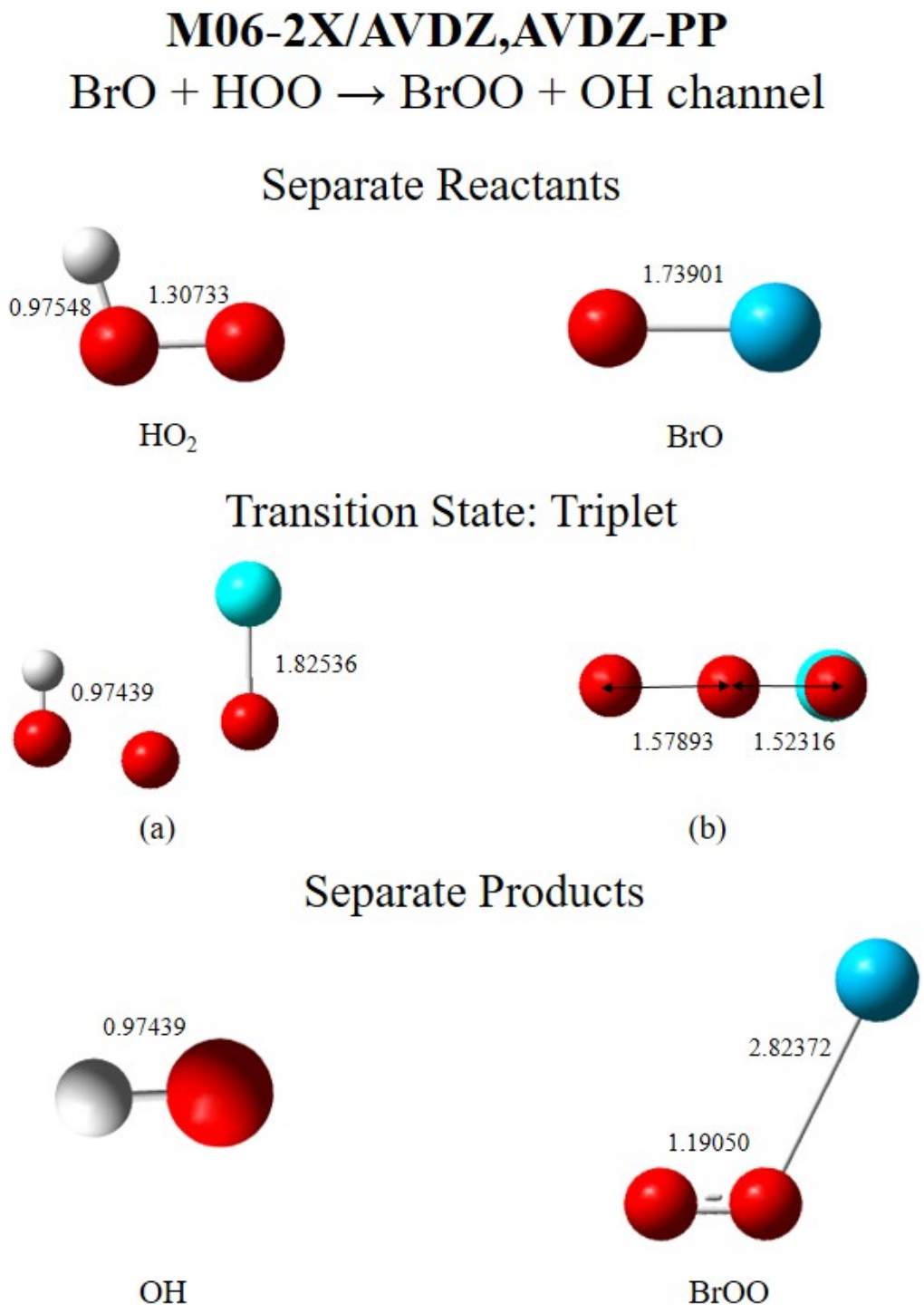
M06-2X/AVDZ,AVDZ-PP
BrO + HOO → BrOO + OH channel
Separate Reactants
0.97548
1.30733
HO2
1.73901
BrO
Transition State: Triplet
0.97439
1.82536
(a)
1.57893
1.52316
(b)
Separate Products
0.97439
OH
2.82372
1.19050
BrOO

Figure S7.

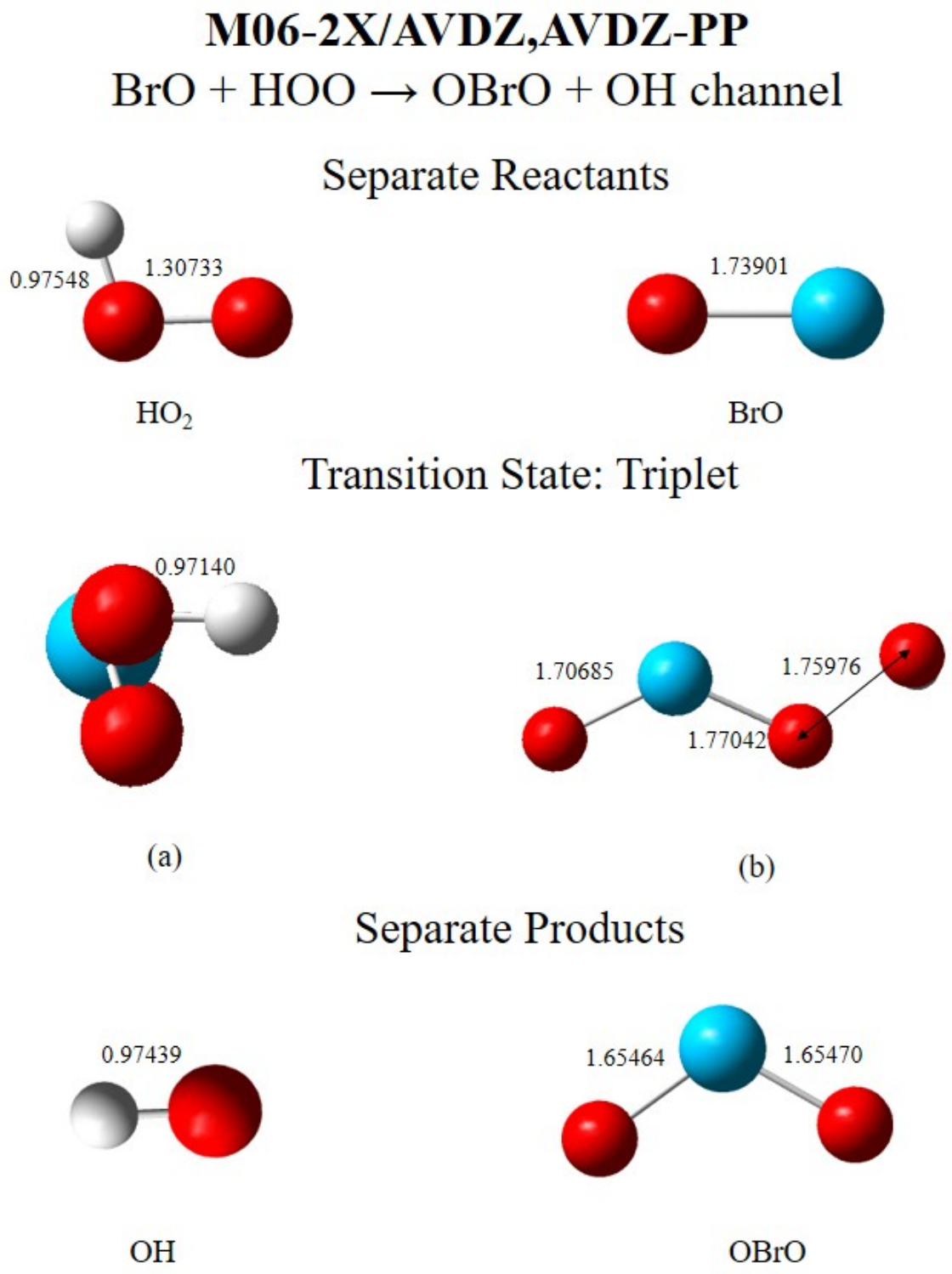
M06-2X/AVDZ,AVDZ-PP
BrO + HOO → OBrO + OH channel
Separate Reactants
0.97548
1.30733
1.73901
HO2
BrO
Transition State: Triplet
0.97140
1.70685
1.75976
1.77042
(a)
(b)
Separate Products
0.97439
1.65464
1.65470
OH
OBrO

Figure S8.

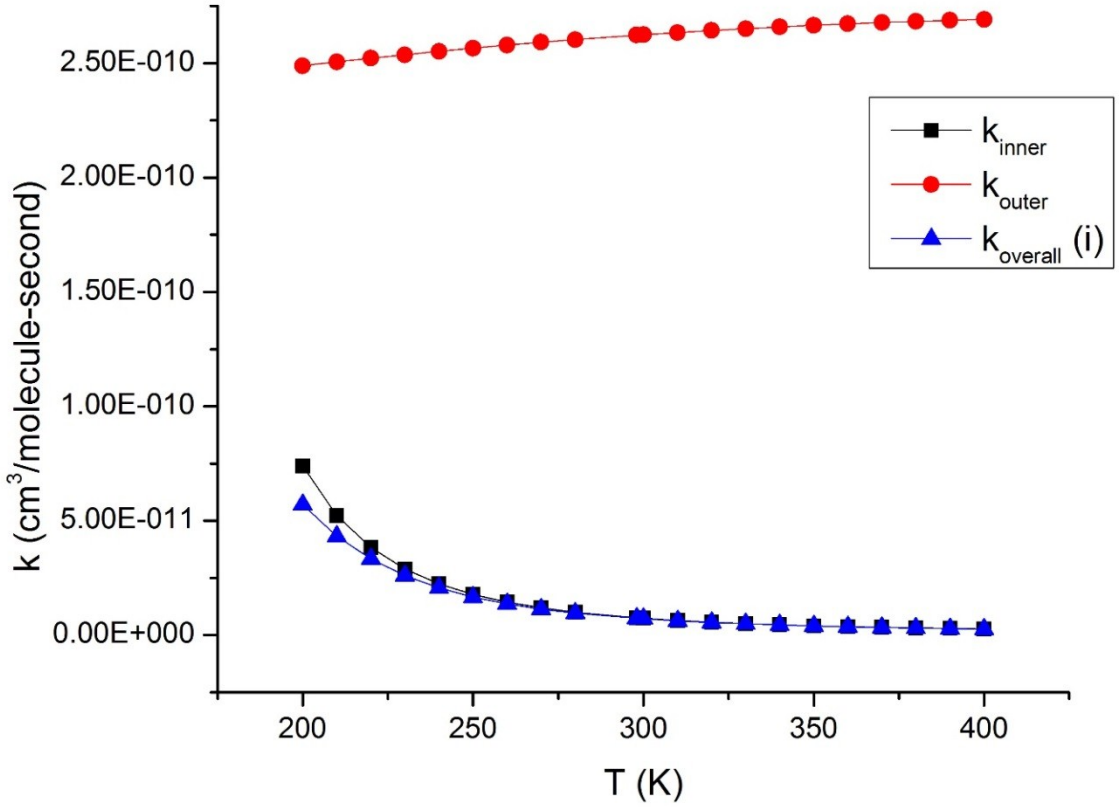
2.50E-010
2.00E-010
1.50E-010
1.00E-010
5.00E-011
0.00E+000
k (cm3/molecule-second)
200
250
300
350
400
T (K)
kinner
kouter
koverall (i)

Figure S9.

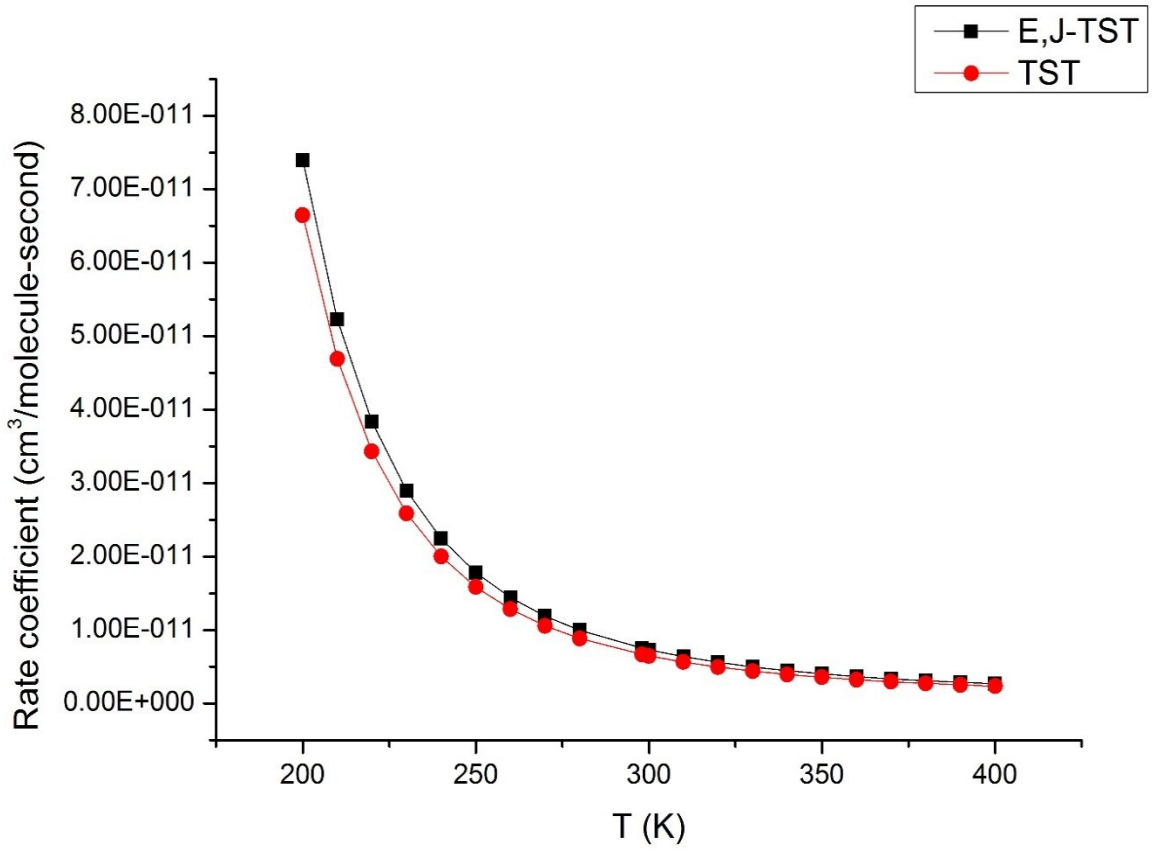
E,J-TST
TST
8.00E-011
7.00E-011
6.00E-011
5.00E-011
4.00E-011
3.00E-011
2.00E-011
1.00E-011
0.00E+000
Rate coefficient (cm3/molecule-second)
200
250
300
350
400
T (K)

Figure S10.

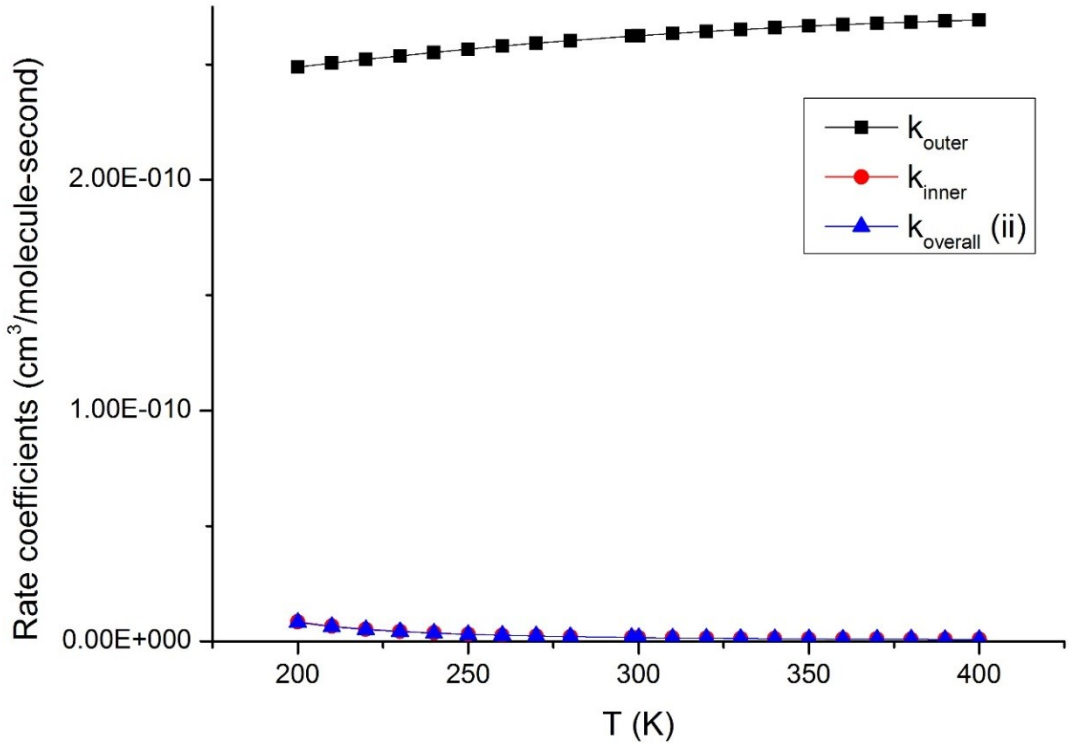
Rate coefficients (cm3/molecule-second)
2.00E-010
1.00E-010
0.00E+000
200
250
300
350
400
T (K)
k outer
k inner
k overall (ii)

Some considerations on the MR characters in the TSs of channel 1(a) and channels 1(b) by CASSCF and/or CASSCF/NEVPT2 calculations

The TS of channel: 1(a)

1. At the M06-2X/AVDZ geometry of the TS of channel 1(a): Some CASSCF/AVDZ calculations with different active spaces were carried out. The computed largest CI coefficients are given below:

CASSCF(2,4):

aa00	0.9999985

CASSCF(4,6):

2aa000	0.9861989
0aa200	-0.1375082
aa0ba0	0.0532421

CASSCF(6,8):

CI vector

22aa0000	0.9820148
20aa2000	-0.1176717
02aa0200	-0.0581623

Conclusion: Although the T1 values obtained from CCSD(T) calculations are large at the M06-2X/AVDZ geometry, CI coefficients obtained from CASSCF calculations with different active spaces suggest that MR character is not very large. In this connection, BD methods are expected to be adequate.

2. At the BD/AVDZ geometry of the TS of channel 1(a): Some RHF/CCSD(T) calculations were carried out on the TS of channel 1(a) at the BD/AVDZ geometry. Although initially there were SCF convergence problems in these RHF calculations, they were overcome by using the CASSCF(2,2) wavefunction as the initial guess for the RHF calculation. Subsequent RHF/CCSD(T) calculations with different basis sets (AVTZ and AVQZ) at the BD/AVDZ geometry with the converged RHF wavefunction give T1 diagnostic values of ~0.053, which is substantially smaller than the values obtained at the M06-2X/AVDZ geometry, suggesting that at the BD/AVDZ geometry, MR character for this triplet TS is acceptably small. In this connection, the BD(T) and BD(TQ) methods are expected to be adequate.

The TS of channel 1(b)

Since the TS structures of channel 1(b) obtained at the M06-2X/AVDZ and BD/AVDZ level are qualitatively similar (as discussed in the paper) and the M06-2X TS geometry gave open-shell singlet states at the BD/AVTZ and BD/AVQZ levels, some CASSCF/NEVPT2 singlet calculations were carried out on the TS of channel 1(b) using MOLPRO at the M06-2X geometry. At the same time, similar CASSCF/NEVPT2 calculations were carried out for the separate reactants at a 50 Å separation in the super molecule approach, in order to obtain the relative energies of the TS with respect to the separate reactants. The CASSF/NEVPT2 results are summarized below.

The CASSCF orbitals and major computed CI vectors from CASSCF(2,4) calculations with different basis sets are very similar. The two highest occupied CASSCF/AVDZ natural orbitals and their electron occupancies are given below:

$(25a)^{1.07}$

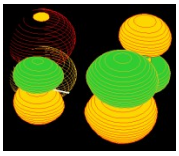

$(26a)^{0.93}$

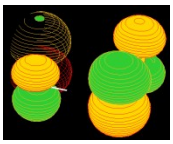

The largest CI coefficients of the open-shell singlet state are:

2000	0.73
0200	-0.68

The computed relative electronic energies (in kcal.mol^{-1}) of the TS of channel 1(b) (w.r.t. separate reactants) obtained at the CASSCF and CASSCF/NEVPT2 levels of calculation with different basis sets are summarized in the following Table:

Basis sets	CASSCF	CASSCF/NEVPT2
AVDZ	8.66	-2.303
AVTZ	9.08	-2.995
AVQZ	9.16	-3.033
CBS($1/X^3$: AVQZ/AVTZ)		-3.062

The best computed NEVPT2/CBS//M06-2X/AVDZ relative energy of -3.06 kcal.mol^{-1} as shown in the above Table agrees almost exactly with the best computed BD(TQ)/CBS//M06-2X/AVDZ value of -3.05 kcal.mol^{-1} (see Table 2 of the paper). In conclusion, single reference BD(TQ)/CBS results and MR CASSCF/NEVPT2 results for channel 1(b) are very consistent. Therefore, for the sake of simplicity and consistency (with other reactions considered in the present investigation), only the BD(TQ)/CBS results are discussed in the paper.